J Therm Anal Calorim (2011) 105:529–534
DOI 10.1007/s10973-011-1562-1

Comparative study of HMX and CL-20

Thermal analysis, combustion and interaction with aluminium

O. Ordzhonikidze · A. Pivkina · Yu. Frolov · N. Muravyev · K. Monogarov

ESTAC2010 Conference Special Issue

Abstract This study deals with a well-known monocyclic nitramine HMX and a relatively new polycyclic strained-cage nitramine CL-20. Experimental data on the powder morphology, simultaneous thermal analysis (STA) and burning rate of binary formulations Al/HMX and Al/CL-20 are presented. Kinetic modelling for HMX and CL-20 are considered based on analysis of STA data obtained for low heating rates. The processing of STA data by the Kissinger method was shown to need to be supplemented with the construction of a thermokinetic model. The thermal decomposition of HMX is reliably described by the reaction of the first order with the autocatalysis. Obtained kinetic parameters of the HMX thermal decomposition correlate with literature-known data on kinetics of the lead stage of HMX combustion. Two types of aluminium powder, i.e. micron-sized and ultrafine, are used to investigate the interaction with both nitramines. Thermal analysis revealed the higher Al oxidation ability of the solid compounds produced at CL-20 thermolysis, than that one of HMX. Burning rate experiments show the differences in the combustion parameters between CL-20- and HMX-based formulations, specifically along with the burn rate level increase for CL-20 monopropellant as compared to HMX one, the pressure exponent and effect of the aluminium particle size variation are also distinct. Results are analyzed and compared to available literature data.

Keywords HMX · CL-20 · Thermokinetic modelling · Thermal analysis

O. Ordzhonikidze (✉) · A. Pivkina · Yu. Frolov · N. Muravyev · K. Monogarov
Semenov Institute of Chemical Physics, Russian Academy of Science, Moscow, Russia
e-mail: olga_ord@mail.ru

Introduction

Nowadays, octahydro-1,3,5,7-tetranitro-1,3,5,7-tetrazocine ($C_4H_8N_8O_8$), known as HMX, is one of the most important energetic ingredients widely used in various propellants and explosives. HMX-based systems have many advantages, i.e. high density, potentially high specific impulse, little smoke produced, as compared to ammonium perchlorate, lower toxicity, and lower corrosion. Being first synthesized in 1987 by Nielsen [1], 2,4,6,8,10,12-hexanitrohexaazaisowurtzitane ($C_6H_6N_{12}O_{12}$, CL-20) is considered to substitute monocyclic nitramines, such as HMX and RDX in high-energy formulations. The cage structure of CL-20 causes additional ring strain, which effects a higher molecular density (438.19 g/mol for CL-20 and 296.16 g/mol for HMX) as well as a significant increase in the heat of formation (415 kJ/mol for CL-20 and 88 kJ/mol for HMX) [2].

Aluminium is one of the main components in propellant; therefore, investigation of Al interaction with HMX and CL-20 is of key importance to meet the advanced performance objectives of solid propellants.

One of methods for investigation of thermal decomposition of energy-intensive substances is a simultaneous thermal analysis (STA), those results are used to develop the global kinetic models of decomposition for both simple matters and energetic condensed systems (ECSs) on basis of them. According to literature data, an experimentally determined value of the activation energy E_a of thermal decomposition of HMX varies from 42 to 1070 kJ/mol [3, 4], and its linear dependence on the logarithm of the pre-exponential factor A for a number of energy-intensive substances (HMX, RDX, NTO etc.) is described by the Brill compensating law [4]. A similar compensating effect was described earlier for dehydration of C_2H_5OH on the

copper catalyst [5] and solid-phase reactions like thermal decomposition of $CaCO_3$ [6] and $MgCO_3$ [7]. For homogeneous reactions and processes in solutions, the compensating effect also is often observed [8] and explained by the constancy of the Gibbs energy ΔG because, with an increase in E_a, the entropy ΔS increases according to

$$\Delta G = E_a - T\Delta S. \quad (1)$$

Vyazovkin and Wight [9] show that, for prevention of uncontrolled heat losses in the course of STA experiment with HMX, it is necessary to use samples with a minimum weight, which are heated with a low rate (about 1 K/min).

The aim of this study is to compare the thermal behaviour and kinetic parameters of two investigated nitramines and their oxidation ability in binary systems with aluminium.

Experimental

Materials and equipment

The materials used in this study were micron-sized HMX (β-polymorph, determined by XRD in our previous work [10]), micron-sized CL-20 (ε-polymorph). SEM images of investigated nitramine powders are shown in Fig. 1 (Quanta 200 3D, FEI, The Netherlands).

To investigate oxidizing ability of nitramines, binary systems with 25 wt% aluminium were studied. Two types of powder were used: micron-sized ASD-6 (average surface diameter $D_S = 1.6$ μm, metal content—95%) and ultrafine ALEX^{TM} ($D_S = 190$ nm, activity—84%), both spherical (other details in [10]).

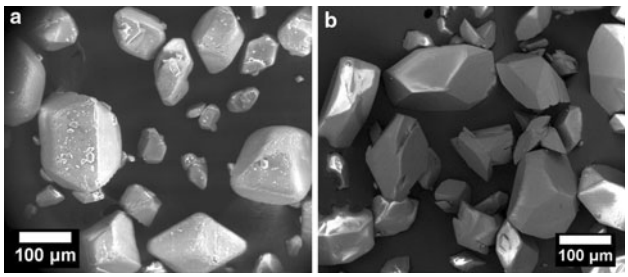

Fig. 1 SEM images of the: **a** HMX and **b** CL-20

Investigation of thermal behaviour was carried out using simultaneous thermal analyzer (STA 449 F3, Netzsch, Germany). For HMX- and CL-20-based samples with mass ~2 mg and heating rates 0.5–20 K/min, experiments in closed alumina pans with pierced lids under dynamic argon flow (70 mL/min) were performed. STA data were processed with Netzsch Proteus—Thermokinetics software (Netzsch, Germany).

Standard techniques were used to measure the burn rate; digitized pressure–time signal and high-speed video recording (1200 fps, Casio EX-F1, Japan) with accuracy ±5% were employed. Measurements were performed using a constant pressure bomb (volume 1.5 l) under nitrogen atmosphere. The sample pellets were cylindrical (8 mm in diameter), fabricated by cold isostatic pressing at 350 MPa during 3 min and coated on the lateral surface with poxipol.

Results and discussion

Thermal analysis of nitramines

The thermal analysis of HMX (Fig. 2a) reveals the presence of two endothermic processes, specifically, the phase change $\beta \rightarrow \delta$ HMX (peak temperature of 191 °C) and melting (279 °C) and the subsequent exothermic decomposition (283 °C). In contrast to the thermal analysis of HMX, the same for CL-20 does not reveal melting the substance (Fig. 2b). On the curve of the differential scanning calorimetry (DSC), we observe the endothermic peak (172 °C) corresponding to the phase change $\varepsilon \rightarrow \gamma$ CL-20 and the exothermic peak of the thermal decomposition of CL-20 (244 °C).

Many researchers [11, 12] believe that the thermal decomposition of both HMX and CL-20 begins from the homolysis of a weakest bond in the N–NO_2 molecule. According to quantum-chemical calculations, the N–NO_2 bond strength in the HMX molecule is 200.9 kJ/mol [13]. From the thermochemical evaluation of corresponding

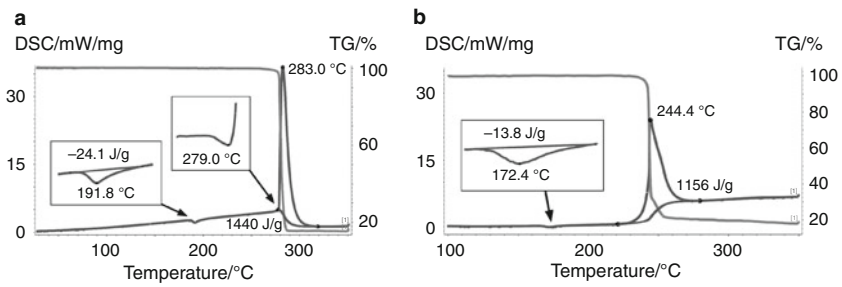

Fig. 2 DSC/TG curves for HMX (**a**) and CL-20 (**b**), heating rate 10 K/min

kinetic parameters, authors [14] obtain $E_a = 193.4$ kJ/mol and $A = 10^{16.42}$/s.

The kinetic parameters (E_a, A) were determined with a model-independent analysis by the Kissinger method (ASTM E698) [15] (Table 1).

In accordance with the results of the analysis of experiments, in all an investigated range of heating rates (0.5–20 K/min), the parameters are 354 kJ/mol and 10^{32}/s, respectively. The values obtained are conservative with the evidence of high error in describing experimental points by the linear dependence (Fig. 3, Table 1). Kinetic parameters obtained at high heating rates reflect the presence, parallel with chemical processes, of physical ones (melting and local overheating of the sample), as was also concluded in [16].

For better result accuracy, all the TG were divided by two ranges, specifically, with low (0.5, 1, and 2 K/min) and high (5, 10, and 20 K/min) rates of heating, and each of them were approximated by its linear dependence. The similar procedure was performed also with TG data for CL-20. It is significant that, with a decrease in heating rates, a value of the activation energy for both HMX and CL-20 decreases and verges towards a value of the N–NO_2 bond breaking energy [17]. To compare the results obtained, Table 1 also lists current literature data.

Thermokinetic modelling of the thermal HMX and CL-20 decomposition, which was carried out based on TG data obtained on heating with rates of 0.5, 1 and 2 K/min, showed that thermolysis is sufficiently described by the first-order reaction with auto-catalysis.

$$d\alpha/dt = A\exp(-E_a/RT)\,\alpha(1 + k_{cat}b) \quad (2)$$

where $\alpha = (m_0 - m)/(m_0 - m_\infty)$ is the substance conversion level; m_0 is the initial weight of a sample; m is the current weight of the sample; m_∞ is the final weight of the sample; $A = 10^{14}$/s is the pre-exponential factor; $E_a = 191.45$ kJ/mol is the activation energy; $k_{cat} = 10^{2.47}$ is the catalysis coefficient; and b is the concentration of final products. Equation 2 for the decomposition rate of HMX can be presented as:

$$d\alpha/dt = 1016.44\exp(-191454/RT)\,\alpha(1 - \alpha) \quad (3)$$

Figure 4 demonstrates dependences of sample weights on the time of their heating with the different rates. The coefficient of the correlation of obtained dependences with the experimental TG data is high—0.9985.

Figure 5 shows the comparison of the kinetic parameters for thermal decomposition of HMX in the dynamic heating mode with rates of 0.5, 1 and 2 K/min that were obtained by the Kissinger method (line 2) and by thermokinetic modelling (line 1) with the parameters [20] determined for combustion (line 3).

In study [20] to obtain the rate constant for the leading reaction of HMX combustion, authors used a Zel'dovich model [21] with the burning rates and surface temperatures, experimentally determined at different pressures:

Table 1 Kinetic parameters for thermal decomposition of HMX and CL-20

Sample	Heating rates/K/min	Kinetic parameters	
		E/kJ/mol	Log (*A*)/s^{-1}
HMX			
1a	5, 10, 20	572 ± 9	52
2a	0.5–20	428 ± 49	39
3a	0.5, 1, 2	207 ± 31	17
	[18]	184	16
CL-20			
1b	5, 10, 20	302 ± 46	29
2b	0.5–20	252 ± 12	24
3b	0.5, 1, 2	190 ± 5	17
	[19]	189 ± 11	18

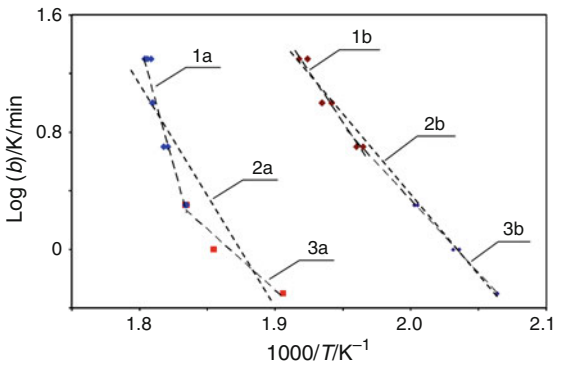

Fig. 3 Logarithm of the heating rate versus the inverse of the temperature at the maximum reaction rate (Kissinger plot) for HMX (*a*) and CL-20 (*b*). (*1*) 5–20; (*2*) 0.5–20; and (*3*) 0.5–2 K/min

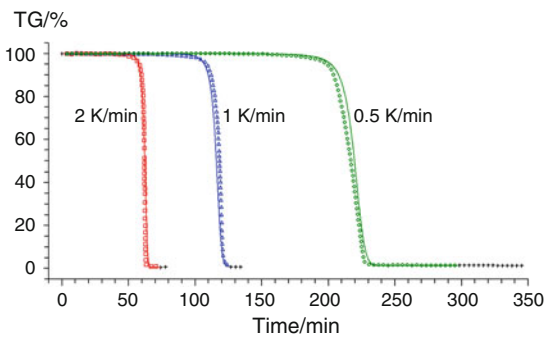

Fig. 4 Results of modelling the thermal decomposition of HMX by the first-order self-catalyzed reaction. *Solid lines* are calculated value and points are TG data

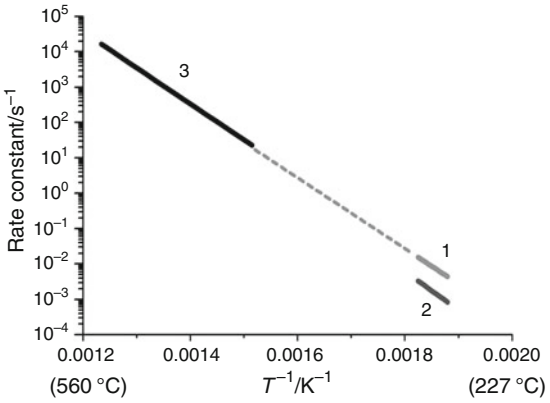

Fig. 5 Comparison of the kinetic parameters for the thermal decomposition of HMX (*line 1*—thermokinetic modelling; *line 2* model-independent Kissinger analysis) with data [20] derived from combustion (*line 3*)

$$m^2 = \frac{2\rho^2 \chi Q}{c_p\left(T_s - T_0 + L_m/c_p\right)^2}\left(\frac{RT_s^2}{E}\right)A\exp(-E/RT_s) \qquad (4)$$

where m is the mass burning rate; c_p is the specific heat capacity; ρ is the density; χ is the heat conductivity coefficient for the condensed phase; T_s is the surface temperature; Q is the heat release on the surface; E_a is the activation energy; and A is the pre-exponential factor for the leading stage of combustion in the condensed phase. The expression $(T_s - T_0 + L_m/c_p)$ determines the warming-up of the condensed phase from initial temperature T_0 to surface temperature T_s with allowance for melting and phase transition heat L_m.

From Fig. 5, it follows that (i) extrapolation of data, obtained under thermal analysis, in the region of the combustion surface temperatures leads to the satisfactory fit; and (ii) the analysis of results by the Kissinger method should be supplemented with thermokinetic modelling to obtain more correct data.

Thermal analysis of nitramine/Al interaction

To investigate the thermal behaviour of metal-nitramine formulations, DSC experiments were conducted. Figure 6 shows DSC curves obtained during constant rate heating of two samples with equal mass of 2 mg: dispersed particles of mixtures 25%ALEX/75%HMX and 25%ALEX/75%CL-20. In thermograms, nitramine decomposition peaks (HMX—284 °C, CL-20—243 °C) and metal melting were observed. In contrast with HMX, for CL-20-based system the clearly marked exothermic peak occurs near the Al melting temperature, which reveals the partial aluminium oxidation by remaining condensed products of the CL-20 thermal decomposition.

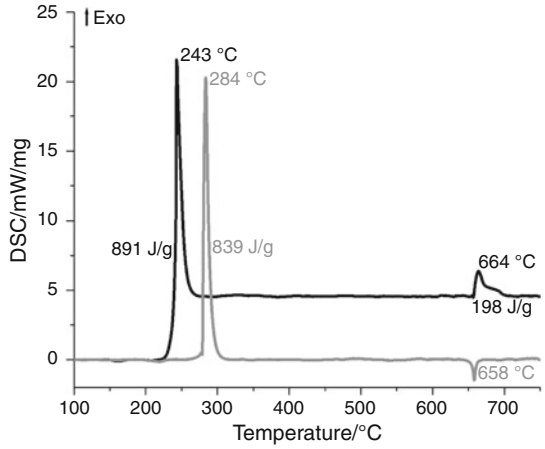

Fig. 6 DSC curves: *grey* 25%ALEX/75%HMX and *black* 25% ALEX/75%CL-20 (10 K/min, argon)

Burning rate of binary compositions Al/nitramine

HMX-monopropellant's burning rate U data as a function of pressure P are plotted in Fig. 7 (curve 1), as was previously presented in [10]. CL-20-monopropellant samples were fabricated by the same technique; however, during combustion under pressure above 3 MPa, coating was cracked; such accelerated (anomalous) burn rates are not shown on Fig. 7. Instead, we plot the line $U(P)$ representing CL-20-monopropellant data reported by Sinditskii et al. [22]. Our data obtained at 3.5 MPa correlate with these data.

The pressure exponent value for CL-20 is lower than that one of HMX (0.78 and 0.93, respectively), whereas the burning rate is about twice higher, as indicated in Table 2.

To investigate the oxidizing ability of two nitramines in the combustion regime, binary formulations with 25 wt% aluminium were examined. Table 2 and Fig. 7 summarize the burning law parameters $U(\text{mm/s}) = B^*P(\text{MPa})^v$ alone

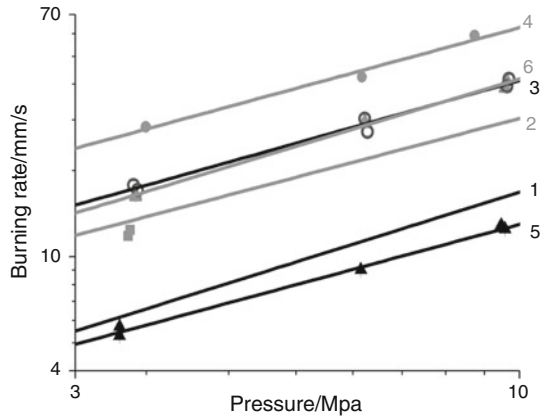

Fig. 7 Burning rates for HMX/CL-20-based systems: *1* HMX, *2* CL-20, *3* ALEX/HMX, *4* ALEX/CL-20, *5* ASD-6/HMX, and *6* ASD-6/CL-20

Table 2 Burning law parameter (B) and pressure exponent (v) for investigated systems with porosity (Π)

N	Composition	B	v	R^2	Π/%
1	HMX	2.0	0.93	0.976	7
2	CL-20 [22]	5.1	0.78		5–10
3	ALEX/HMX	6.1	0.83	0.987	12
4	ALEX/CL-20	9.9	0.81	0.984	6
5	ASD-6/HMX	2.1	0.8	0.993	7
6	ASD-6/CL-20	5.3	0.89	0.996	3

with the correlation coefficients R^2 and average samples porosities of the samples Π for monopropellants and binary formulations. Both the micron and ultrafine aluminium enhance the burning rate of CL-20 (curves 6 and 4, Fig. 7). In contrast, the effect of micron-Al addition to HMX appears to retard the burn rate (curve 5), whereas ultrafine metal considerably increases U value (curve 3). The influence of aluminium particle size is expected: the smaller particles, the greater combustion velocity. The highest U values are measured for ALEX/CL-20 formulation. In general, CL-20-based systems have higher burning rates, than that ones of HMX with Al of the same powder grade.

Effect of the aluminium addition results in a pressure exponent v decreasing for HMX-based compositions from 0.93 for neat HMX to 0.80 for ASD-6/HMX, whereas for CL-20-based formulations it even increases v from 0.78 for neat CL-20 to 0.89 for ASD-6/CL-20.

Conclusions

Thus, in this study, two different approaches to kinetic modelling the TG data for HMX and CL-20 were considered, specifically, (i) the analysis of data obtained in the whole range of heating rates and (ii) single modelling for both low- and high-rate ranges. The value of the activation energy obtained at low rates of heating corresponds to the N–NO_2 bond breaking energy, which is postulated as the first stage of the reaction for both the substances. It was shown that Kissinger analysis of STA data need to be supplemented with the construction of a thermokinetic model. The thermal decomposition of HMX and CL-20 is reliably described by the reaction of the first order with the autocatalysis, and the kinetic parameters obtained correlate with literature-known data on kinetics of the leading stage of these nitramines combustion.

The ability of solid products of HMX and CL-20 pyrolysis to oxidize metal aluminium was examined by STA and by the burn rate measurements. DSC results revealed that CL-20 solid products are much more oxidative resulting in Al oxidation at melting point, whereas HMX products do not oxidize Al under thermal analysis confinement. Burn rate data of neat nitramines show considerable enhancement of CL-20 combustion velocity as compared to HMX. This tendency remains when aluminium powder is added to nitramines, i.e. CL-20-based systems have higher burning rates, than that ones of HMX with Al of the same powder grade. However, there is a remarkable difference in the aluminium particle size effect on the nitramine's combustion: both the micron- and ultra-sized aluminium enhance the burning rate of CL-20, whereas the effect of micron-Al addition to HMX appears to retard the burn rate, although ultrafine ALEX considerably increases U value.

Future study includes investigation of the combustion residue collected from the combustion surface to determine the combustion completeness and estimate agglomeration phenomena. Direct observations of the combustion surface dynamics with the high-speed video recording would be useful to study the mechanism of the nitramine interaction with aluminium during combustion wave propagation.

Acknowledgements Financial support of the Russian Foundation of Basic Research (RFFI grant #10-03-00317a) is gratefully acknowledged.

References

1. Nielsen AT. Synthesis of polynitropolyaza caged nitramines chemical propulsion information agency; 1987, Publication no. 473.
2. Lobbecke S, Bohn MA, Pfeil A, et al. Thermal behavior and stability of HNIW (CL 20). In: Proceedings of the 29th International Annual Conferrence on ICT, Karlsruhe; 1998. p. 145/1–145/15.
3. Kimura J, Kubota N. Thermal decomposition process of HMX. Propell Expl Pyrotech. 1980;5(1):1–8.
4. Brill TB, Gongwer PE, Williams GK. Thermal decomposition of energetic materials 66. Kinetic compensation effects in HMX, RDX and NTO. J Phys Chem. 1994;98(47):12242–7.
5. Constable FH. The mechanism of catalytic decomposition. Proc R Soc Lond. 1925;108:355–78.
6. Gallagher PK, Johnson DW. Kinetics of the thermal decomposition of CaCo3 in Co2 and some observations on the kinetic compensation effect. Thermochim Acta. 1976;14:255–61.
7. Dollimore D, Rodgers PF. The appearance of a compensation effect in the thermal decomposition of manganese(II) carbonates, prepared in the presence of other metal ions. Thermochim Acta. 1979;30(1):273–80.
8. Leffler JE, Grunwald E. Rates and equilibria of organic reactions. New York: Wiley; 1963.
9. Vyazovkin S, Wight CA. Kinetics in solids. Annu Rev Phys Chem. 1997;48:125–49.
10. Muravyev N, Frolov Yu, Ordzhonikidze O, et al. Particle size and mixing technology influence on combustion of HMX/Al compositions. In: Proceedings of the 36th International Pyrotechnic Seminar, Rotterdam; 2009. p. 43.
11. Bulusu S, Behrens RA. Review of the thermal decomposition pathways in RDX, HMX and other closely related cyclic nitramines. Def Sci J. 1996;46(5):347–60.

12. Geetha M, Nair UR, Sarwade DB, et al. Studies on CL-20: the most powerful high energy material. J Therm Anal Calorim. 2003;73:913–22.
13. Melius SF. Thermochemical modeling: II. Application to ignition and combustion of energetic materials. In: Bulusu S, editor. Chemistry and physics of energetic materials. Boston: Kluwer; 1990. p. 51–78.
14. Shaw R, Walker FE. Estimated kinetics and thermochemistry of some initial unimolecular reactions in the thermal decomposition of l,3,5,7-Tetranitro-l,3,5,7-tetraazacyclooctane in the gas phase. J Phys Chem. 1977;81:2572–6.
15. Kissinger HE. Reaction kinetics in differential thermal analysis. J Anal Chem. 1957;29(11):1702–6.
16. Pinheiro GFM, Lourenco VL, Iha K. Influence of the heating rate in the thermal decomposition of HMX. J Therm Anal Calorim. 2002;67:445–52.
17. Brill TB, Karpowicz RJ. Solid phase transition kinetics: the role of intermolecular forces in the condensed-phase decomposition of octahydro-1,3,5,7-tetranitro-1,3,5,7-tetrazocine. J Phys Chem. 1982;86(21):4260–5.
18. Tarver CM, Tran TD. Thermal decomposition models for HMX-based plastic bonded explosives. Combust Flame. 2004;137(1–2): 50–62.
19. Korsounskii BL, Nedelko VV, Chukanov NV, et al. Kinetics of thermal decomposition of hexanitrohexazaisowurtzitane. Russ Chem Bull. 2000;49(5):812–8.
20. Sinditskii VP, Egorshev VY, Serushkin VV, et al. Evaluation of decomposition kinetics of energetic materials in the combustion wave. Thermochim Acta. 2009;496(1–2):1–12.
21. Zeldovich YB. Theory of combustion of propellants and explosives. Zh Eksp Teor Fiz. 1942;12(11–12):498–524.
22. Sinditskii VP, Egorshev VY, Berezin MV, et al. Study on combustion of energetic cyclic nitramines. Zh Khim Fiz. 2003;22(7): 64–9.